J. Fluid Mech. (1975), *vol.* 69, *part* 3, *pp.* 615–624
Printed in Great Britain

A viscous internal wave in a stratified fluid whose buoyancy frequency varies with altitude

By D. GORDON, U. R. KLEMENT AND T. N. STEVENSON
Department of the Mechanics of Fluids, University of Manchester, England

(Received 17 October 1974)

A viscous incompressible stably stratified fluid with a buoyancy frequency which varies slowly with altitude is considered. A simple harmonic localized disturbance generates an internal wave in which the energy propagates along curved paths. Small amplitude similarity solutions are obtained for two-dimensional and axisymmetric waves. It is found that under certain conditions the wave amplitude can increase with height. The two-dimensional theory compares quite well with experimental measurements.

1. Introduction

An internal gravity wave is produced in a stably stratified fluid when a localized disturbance oscillates at a frequency equal to or less than ω_0, the buoyancy or Brunt–Väisälä frequency of the fluid. Görtler (1943) showed that the energy propagates along the arms of a cross inclined at angles of $\sin^{-1}(\omega/\omega_0)$ to the horizontal, where ω is the oscillatory frequency of the disturbance. The arms of the cross are straight when ω_0 is constant and curved when ω_0 varies with altitude. The effects of viscosity on a two-dimensional wave in an incompressible fluid which has a constant buoyancy frequency were studied by Thomas & Stevenson (1972). They obtained a similarity solution which shows how the width of the wave increases away from the disturbance. This paper will be referred to as I.

In the present paper the theory of I is extended to two- and three-dimensional waves in a fluid with a buoyancy frequency which varies slowly with altitude. The theory is compared with experimental measurements in two-dimensional waves. When ω_0 varies with height the oscillations within the wave can increase in amplitude with height even though the kinematic viscosity remains constant, whereas when ω_0 remains constant the wave amplitudes always attenuate.

2. Two-dimensional theory

A stratified incompressible fluid in which the background density and viscosity are, for the present, unspecified is considered. A solution for the flow field around a horizontal line disturbance is sought in a vertical plane which is perpendicular to the line disturbance. The disturbance is simple harmonic with frequency ω. Only one arm of the cross is considered.

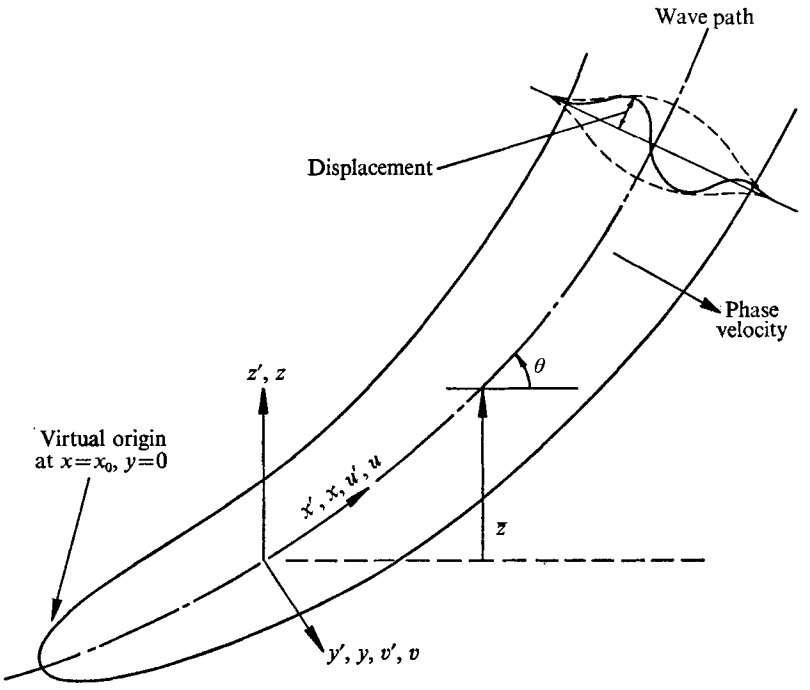

FIGURE 1. Co-ordinate axes.

Experiments show that the energy lies in a narrow region centred about a wave path $\theta = \theta(x')$, where θ is the angle of the wave path to the horizontal. The x' co-ordinate is measured along the wave path from an origin which is near the mean position of the disturbance and the y' co-ordinate is normal to the wave path and in the direction of the inviscid phase velocity (see figure 1). The curve $\theta = \theta(x')$ will be related to the buoyancy frequency in the subsequent analysis.

The velocity components are u' and v', ρ_T is the density, μ_T the viscosity, p_T the pressure and t' is the time. The perturbation variables are $p' = p_T - p_0$, $\rho' = \rho_T - \rho_0$ and $\mu' = \mu_T - \mu_0$, where the subscript zero refers to the equilibrium values.

Experimental measurements in the wave indicate that the u' velocity components are much larger than the v' velocity components and that the variations with y' are much greater than those with x'. The dimensionless variables (undashed) are defined as follows:

$$x' = x/\beta, \quad y' = y\alpha/\beta, \quad u' = ua g/\omega, \quad v' = v\alpha a g/\omega,$$

$$t' = t/\omega, \quad \rho' = \rho a \rho^*, \quad \mu' = \mu a \mu^*, \quad p' = p\alpha a \rho^* g/\beta,$$

where $\alpha = (\beta^2\mu^*/2\rho^*\omega)^{\frac{1}{3}}$, $\beta = \omega^2/g$ and g is the gravitational acceleration. μ^* and ρ^* are the constant equilibrium conditions at the level of the disturbance and a is a constant amplitude coefficient. Following I it will be assumed that θ is not close to 0 or $\frac{1}{2}\pi$ and that $a \ll \alpha \ll 1$ so that terms involving a may be neglected

relative to terms involving α. Thus the continuity and incompressibility equations in non-dimensional form with curvilinear co-ordinate scale factors (h, 1) are

$$\frac{\partial u}{\partial x}+\frac{\partial}{\partial y}(hv)=0 \tag{1}$$

and
$$\partial\rho/\partial t=\lambda_0 r_0(u\sin\theta-\alpha v\cos\theta), \tag{2}$$

where
$$h=1+\alpha y\,d\theta/dx,\quad \lambda_0=\beta_0/\beta,\quad r_0=\rho_0/\rho^*.$$

The perturbation momentum equations obtained by subtracting the hydrostatic relations are

$$r_0\frac{\partial u}{\partial t}=-\frac{\alpha}{h}\frac{\partial p}{\partial x}-\rho\sin\theta+2\alpha\left\{m_0\frac{\partial}{\partial y}\left(\frac{1}{h}\frac{\partial}{\partial y}(hu)\right)+\frac{\partial m_0}{\partial y}\frac{\partial u}{\partial y}\right\}+O(a)+O(\alpha^2) \tag{3}$$

and
$$r_0\alpha\,\partial v/\partial t=-\partial p/\partial y+\rho\cos\theta+O(a)+O(\alpha^2), \tag{4}$$

where $m_0=\mu_0/\mu^*$. The boundary conditions to be satisfied are that the dependent variables u, v, ρ and p and all their derivatives tend to zero as $y\to\pm\infty$.

The dimensionless vertical co-ordinate z ($=z'\beta$) is written as (see figure 1)

$$z=\bar{z}(x)-\alpha y\cos\theta(x), \tag{5}$$

where
$$\bar{z}(x)=\int_0^x\sin\theta(k)\,dk. \tag{6}$$

m_0, r_0 and λ_0 are functions of z and may be expanded in powers of α. Thus

$$r_0(z)=r_1(x)+\alpha r_2(x,y)+O(\alpha^2),$$

where
$$r_1(x)=r_0(\bar{z})\quad\text{and}\quad r_2(x,y)=-y\cos\theta\,dr_0(\bar{z})/dz.$$

Similarly

$$\lambda_0(z)=\lambda_1(x)+\alpha\lambda_2(x,y)+O(\alpha^2)\quad\text{and}\quad m_0(z)=m_1(x)+\alpha m_2(x,y)+O(\alpha^2).$$

It is assumed that the perturbation variables have a time dependency e^{-it} and may be expanded as $u=u_1+\alpha u_2\ldots$, $v=v_1+\alpha v_2\ldots$, $p=p_1+\alpha p_2\ldots$, and $\rho=\rho_1+\alpha\rho_2\ldots$. These are substituted into (1)–(4) and terms of like order are equated to give

$$\partial u_1/\partial x+\partial v_1/\partial y=0, \tag{7}$$

$$\rho_1=i\lambda_1 r_1 u_1\sin\theta=ir_1u_1/\sin\theta, \tag{8}$$

$$i\rho_2+u_1\sin\theta(\lambda_2 r_1+\lambda_1 r_2)+\lambda_1 r_1(u_2\sin\theta-v_1\cos\theta)=0, \tag{9}$$

$$ir_2u_1+ir_1u_2-\partial p_1/\partial x-\rho_2\sin\theta+2m_1\,\partial^2u_1/\partial y^2=0 \tag{10}$$

and
$$\rho_1\cos\theta-\partial p_1/\partial y=0. \tag{11}$$

Equation (8) gives the wave path in terms of the background conditions:

$$\theta(x)=\sin^{-1}(\lambda_1^{-\frac{1}{2}})=\sin^{-1}(\omega/\omega_0). \tag{12}$$

$x(\bar{z})$ may be written in terms of the background density r_0 as

$$x(\bar{z})=\int_0^{\bar{z}}\left(-\frac{1}{r_0}\frac{dr_0}{dz}\right)^{\frac{1}{2}}dz. \tag{13}$$

The analysis now follows that of I and will merely be outlined. It is convenient to introduce the dimensionless variable $P(x,y,t) = (r_1 \cot\theta)^{-\frac{1}{2}} p_1$. An equation for P is then obtained from (7)–(11) together with the stipulated boundary conditions:

$$\frac{\partial P}{\partial x} + \left\{\frac{d}{dx}(\log\sin\theta)\right\} y\frac{\partial P}{\partial y} + \left(i\frac{m_1}{r_1}\tan\theta\right)\frac{\partial^3 P}{\partial y^3} = 0. \tag{14}$$

This equation is essentially the x-direction momentum equation and the momentum flux condition may be found by integrating it across the wave path from $y = -\infty$ to $+\infty$:

$$\frac{\partial}{\partial x}\left(\int_{-\infty}^{\infty} P\,dy\right) - \left(\frac{d}{dx}\log\sin\theta\right)\int_{-\infty}^{\infty} P\,dy = 0,$$

provided that

$$[yP]_{-\infty}^{\infty} = 0, \quad \left[\frac{\partial^2 P}{\partial y^2}\right]_{-\infty}^{\infty} = 0. \tag{15}$$

In this case

$$\int_{-\infty}^{\infty} P\,dy = J\sin\theta\, e^{-it}, \tag{16}$$

where J is a constant.

The solution to (14) must satisfy the momentum flux condition and the boundary conditions at $y = \pm\infty$, including conditions (15). P is assumed to be of the form

$$P = l(x) f(\eta)\, e^{-it},$$

where $\eta = y/b(x)$. Equation (14) now reduces to the ordinary differential equation

$$3f''' + i(\eta f' + f) = 0, \tag{17}$$

and the momentum flux condition reduces to

$$\int_{-\infty}^{\infty} f\,d\eta = J,$$

providing

$$b(x) = \sin\theta(x)\left\{\int_{x_0}^{x} \frac{m_1(k)\tan\theta(k)}{r_1(k)\sin^3\theta(k)}\,dk\right\}^{\frac{1}{3}} \tag{18}$$

and

$$l(x) = \left\{\int_{x_0}^{x} \frac{m_1(k)\tan\theta(k)}{r_1(k)\sin^3\theta(k)}\,dk\right\}^{-\frac{1}{3}}. \tag{19}$$

The point $x = x_0$ is for the moment arbitrary, but represents the position from which the internal wave originates. At this point, which is referred to as the virtual origin of the wave, $b(x) = 0$. Equation (17) is the same as that obtained in I and the solution satisfying the boundary conditions and the momentum flux condition is

$$f = \int_0^{\infty} \exp(-\kappa^3 + i\kappa\eta)\,d\kappa. \tag{20}$$

The dimensionless variables take the following forms:

$$p_1 = \mathscr{R}(l(r_1\cot\theta)^{\frac{1}{2}} f e^{-it}), \tag{21}$$

$$u_1 = \mathscr{R}\left(-\frac{il}{b}(r_1\cot\theta)^{-\frac{1}{2}}\frac{df}{d\eta}e^{-it}\right), \tag{22}$$

$$v_1 = \mathscr{R}\left\{i\left[\frac{l}{b}\frac{db}{dx}(r_1\cot\theta)^{-\frac{1}{2}}\eta\frac{df}{d\eta} - \frac{d}{dx}(l(r_1\cot\theta)^{-\frac{1}{2}})f\right]e^{-it}\right\}, \tag{23}$$

$$\rho_1 = \mathscr{R}\left(\frac{l}{b\sin\theta}(r_1\tan\theta)^{\frac{1}{2}}\frac{df}{d\eta}e^{-it}\right), \tag{24}$$

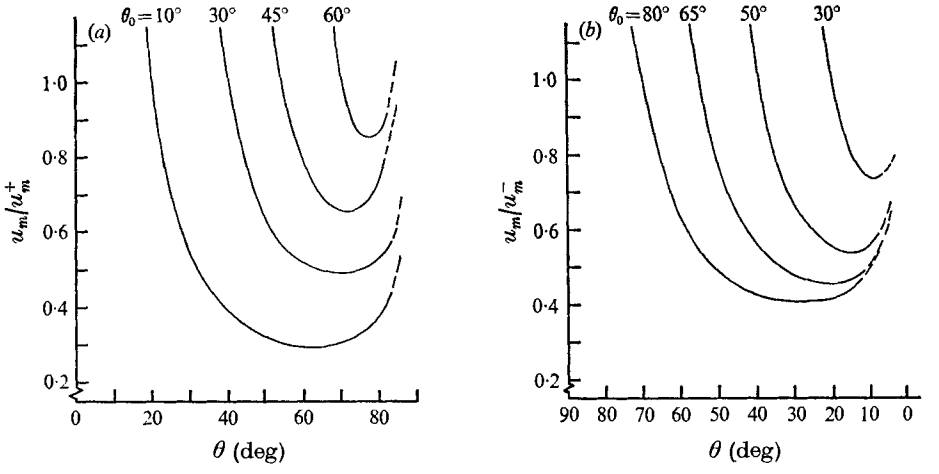

FIGURE 2. The variation in the maximum velocity u_m along the wave path when (*a*) $\theta = \sin^{-1}(Cx^{\frac{1}{3}})$ and (*b*) $\theta = \cos^{-1}(Cx)$. θ_0 is the angle the wave path makes with the horizontal at the virtual origin $x = x_0$. $u_m^{\pm}$ are the values of u_m where $\theta = \theta_0 \pm 10°$.

and the dimensionless displacement δ ($= \delta'\beta/a$) along the wave is given by

$$\delta = \mathscr{R}\left(\frac{l}{b}(r_1 \cot\theta)^{-\frac{1}{2}}\frac{df}{d\eta}e^{-it}\right). \tag{25}$$

These equations describe a narrow region close to the wave path in which energy is propagating away from the disturbance. The width $b(x)$ of the wave is given by (18). Wave crests and troughs lie along lines of constant η and their phase velocity is in the $+y$ direction.

The maximum velocity $u_m(x)$ at the centre of the wave reduces with altitude initially but can eventually increase with altitude if the background conditions are suitable. Under the Boussinesq approximation $r_1 = m_1 = 1$, it can be shown that u_m can increase away from the disturbance if

$$\left(\frac{-3c_1^{\frac{3}{2}}\sin\theta\cos 2\theta}{2^{\frac{5}{4}}\sin^{\frac{3}{4}}2\theta\, u_m^{\frac{3}{2}}}\right)\frac{d\theta}{dx} > 1,$$

where

$$c_1 = \int_0^\infty \kappa \exp(-\kappa^3)\,d\kappa.$$

Consequently an increase in u_m can occur when $0 < \theta < \frac{1}{4}\pi$ if the angle of the wave path to the horizontal decreases sufficiently quickly with altitude. When $\frac{1}{4}\pi < \theta < \frac{1}{2}\pi$ the velocity will increase with altitude only if θ increases sufficiently quickly. Examples of two cases in which the velocities increase are given in figures 2 (*a*) and (*b*), where the wave paths have the forms $\theta = \sin^{-1}(Cx^{\frac{1}{3}})$ and $\theta = \cos^{-1}(Cx)$ respectively. The origin of the disturbance is at $x = x_0$, where $\theta = \theta_0$. The increases in velocity occur as the wave bends towards the vertical and towards the horizontal respectively. When θ is constant u_m always decreases with altitude. It must be noted that the theory cannot be applied close to $\theta = 0$ or $\frac{1}{2}\pi$.

The solution for the axisymmetric wave produced by an oscillating point disturbance is given in the appendix. The magnitudes of the dependent variables are virtually their two-dimensional values divided by the square root of the distance from the axis.

3. Experiments

A glass-sided tank 1·8 m long, 0·9 m high and 0·55 m from front to back was used. The stratification was obtained by filling the tank from the bottom with layers of successively denser salt solution and then allowing the solution to diffuse for two days. A small body was suspended at different heights in the tank. The body was attached to a balance and the different buoyancy forces acting on the body were used to calculate the density distributions.

An internal wave was generated by a 10 mm diameter horizontal cylinder which spanned the tank and oscillated such that its longitudinal axis remained horizontal. Neutrally buoyant oil drops within the wave (see I) were observed using a ciné camera fixed to a traversing system. The ciné camera was synchronized such that the time of each frame in the film was known relative to the time at which the cylinder was in its mean position. The amplitudes within the wave were typically 1 mm.

Waves in two different stratifications are described: one in which the angle θ decreases with altitude (stratification A) and one in which θ increases (stratification B). The experiments will be compared with the Boussinesq form of the equations.

Stratification A

The density distribution within the tank was given by

$$\rho_0/\rho_w = 1{\cdot}14 - Az - Bz^2,$$

where ρ_w is the density of water, $A = 1{\cdot}99$, $B = 27{\cdot}8$ and $z = z'\beta$. The oscillatory frequency ω of the cylinder was 0·88 rad s^{-1} and the wave path calculated from the density distribution is approximately

$$\sin\theta = 1{\cdot}12/(A + 2Bz)^{\frac{1}{2}}. \tag{26}$$

For the experiments the origin of the co-ordinate system is taken as the virtual origin, so that $x_0 = 0$. The value of α was $2{\cdot}3 \times 10^{-3}$ and the amplitude coefficient a was two orders of magnitude less than this.

A virtual origin was chosen to give a reasonable fit with the experiments and this value is used in all the comparisons. Given the wave path, the virtual origin and α, a position in the tank at which measurements were made was transformed from (x', y') to (x, y) and then to (x, η) using the theoretical value of $b(x)$ from (18). The wave path is shown in figure 3, the variation in wave width in figure 4 and the variation in the maximum displacements $\delta'_{\max}$ in figure 5. The curves calculated from the theory are also shown on the figures. Both the theoretical and experimental variations in the phase across the wave relative to the phase at $\eta = 0$ are shown in figure 6.

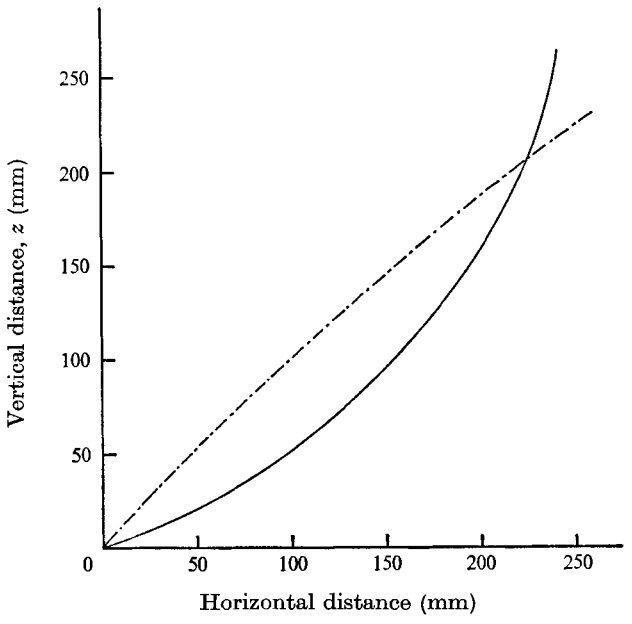

FIGURE 3. The wave path from the virtual origin. – · –, stratification A, equation (26); ——, stratification B, equation (27).

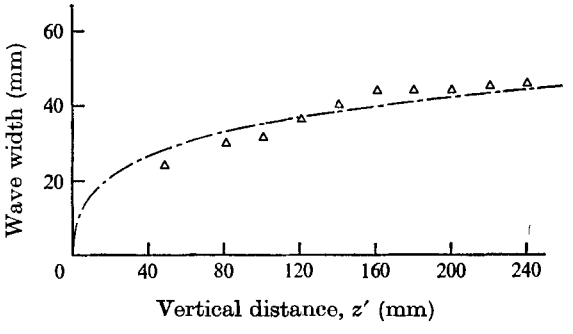

FIGURE 4. Variation in the wave width with height z' for stratification A. The width is measured between the positions at which the maximum displacements are 0·6 of the maximum centre-line displacement. – · –, theory; △, experiment.

Stratification B

In the second set of measurements the wave path had the form

$$\sin\theta = (C+Dz)^{\frac{1}{3}}, \tag{27}$$

where $C = 0{\cdot}0191$ and $D = 28{\cdot}1$. The wave path is shown in figure 3. The oscillatory frequency was $1{\cdot}14\,\mathrm{rad\,s^{-1}}$ and α was $1{\cdot}7\times10^{-3}$. The amplitude coefficient was again two orders of magnitude less than α.

The wave width calculated from (18) is

$$b = \left(\frac{3}{D}\log\left|\frac{\tan(\frac{1}{2}\theta)}{\tan(\frac{1}{2}\theta_0)}\right|\right)^{\frac{1}{3}}\sin\theta$$

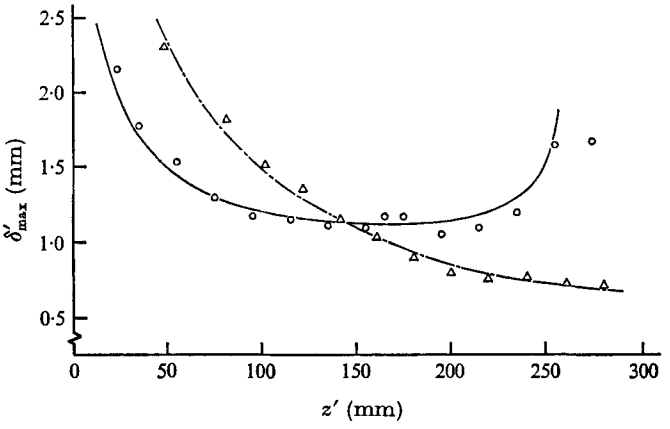

FIGURE 5. The maximum displacements δ'_{max} along the wave from the virtual origin. Stratification A: – · –, theory; △, experiment. Stratification B: ——, theory; ○, experiment.

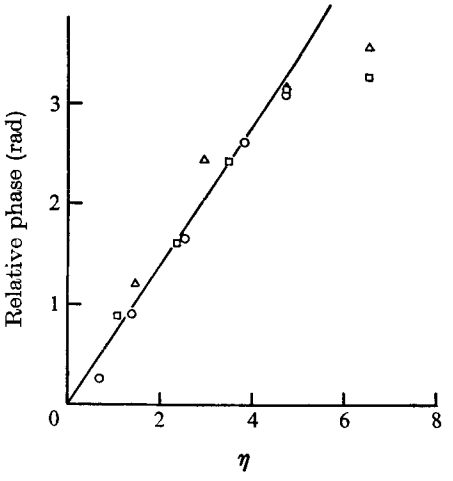

FIGURE 6. The variation in phase across half of the wave relative to the phase at $\eta = 0$ for stratification A. ——, theory. Experiments, distances above the virtual origin: △, $z' = 140$ mm; ○, $z' = 181$ mm; □, $z' = 201$ mm.

and the theoretical maximum displacements at $\eta = 0$ are given by

$$\delta_{max} = c_1(\sin^3\theta/b^4\cos\theta)^{\frac{1}{2}}.$$

The maximum displacements are shown in figure 5 and the variations of the displacements with time are shown in figure 7. The theoretical curves are also shown.

4. Discussion

The closer a wave is to the vertical the smaller is its group velocity, the velocity at which energy propagates along it, and therefore a stronger wave exists in which the amplitudes are higher. An extreme case was described by Gordon &

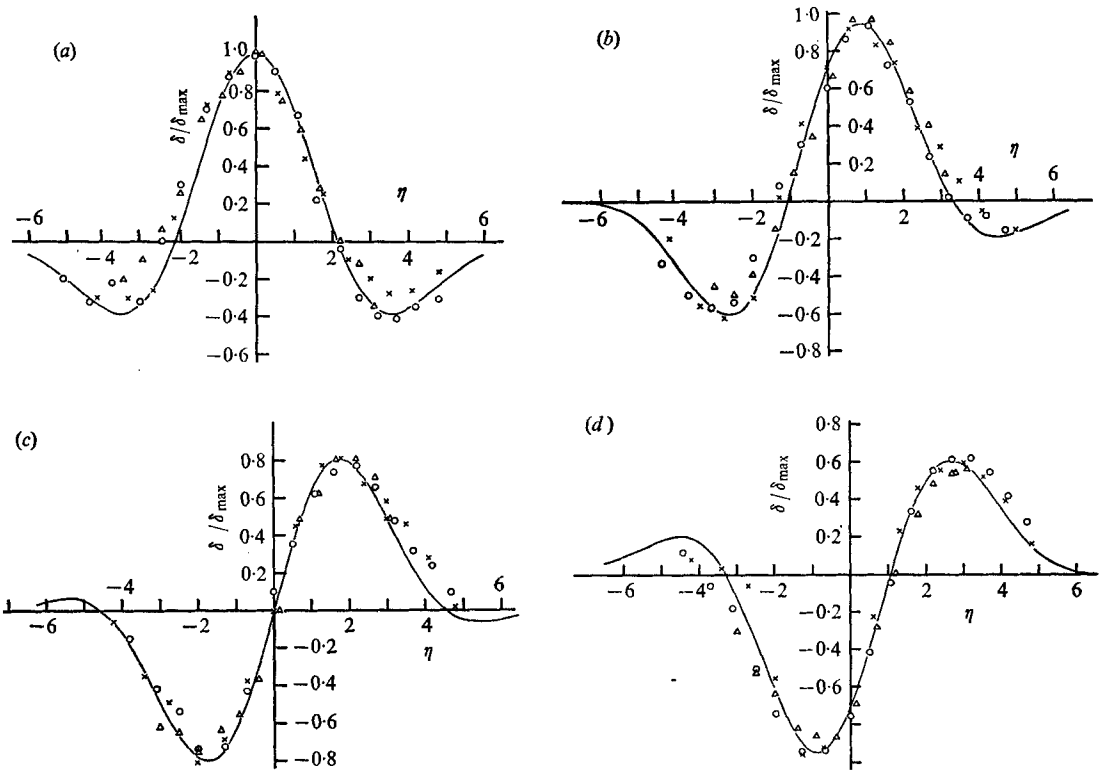

FIGURE 7. A comparison between the experimental and theoretical displacement profiles at four times during a half-cycle for stratification *B*. ——, theory. Experiments, distances above the virtual origin: ×, $z' = 35$ mm; ○, $z' = 75$ mm; △, $z' = 175$ mm. The dimensionless times t: (*a*) $\frac{1}{2}\pi$, (*b*) $\frac{3}{4}\pi$, (*c*) π, (*d*) $\frac{5}{4}\pi$.

Stevenson (1972). They showed that a body oscillating at the buoyancy frequency in a fluid with a constant buoyancy frequency can generate a very strong vertical wave.

The errors introduced by the various approximations within the theory have been estimated in the same manner as that used in I. For stratification *A* the wave has only a small curvature and it appears that all the neglected terms are less than 10 % of those retained for the region in which measurements were taken. This was also the case for the straight wave in I. However, for stratification *B* the large curvature and steep inclination of the wave path do violate some of the theoretical assumptions. The ratio of the nonlinear convection term $u'\,du'/dx'$ to the pressure term $\rho_T^{-1}\,\partial p'/\partial x'$ is less than 0·2 when θ is less than 75° but increases rapidly as θ approaches $\frac{1}{2}\pi$. This restriction could have been reduced by decreasing the amplitude of oscillation within the wave. However the curvature term $\alpha y\,d\theta/dx$ is more restrictive. This term increases in a similar way but at the outer edge of the wave it is greater than 0·2 when θ is above 70°. The ratio $v'_{\text{r.m.s.}}/u'_{\text{r.m.s.}}$ of the theoretical root-mean-square velocities in the y' and x' directions is the most restrictive in that it reaches a value of 0·2 at the outer edge of the wave when θ reaches 68°. The outer edge of the wave was taken as $\eta = 5{\cdot}85$.

Although the experimental results show considerable scatter they do roughly follow the theoretical predictions even when θ is greater than 68°. As the wave turned towards the vertical there was evidence of reflected energy propagating back towards the horizontal level of the disturbance. This was seen as a general increase in the level of the disturbance outside the main wave. However, it was not possible to correlate the results in the reflected wave.

D. Gordon was in receipt of a Scientific Research Council maintenance grant and U. R. Klement a University of Manchester postgraduate award. The work is supported by the Procurement Executive of the Ministry of Defence.

Appendix. The axisymmetric wave

The flow field produced by a vertically oscillating point source is symmetrical about the vertical line through the source, and the region of disturbance is centred about a surface with this vertical line as axis. The wave path is the intersection of this surface with a vertical plane containing the point source. The wave path passes through the mean position of the point source and this is chosen as the origin of the co-ordinate system (x, y, Ω). x is measured along the wave path and y is normal to it as in the two-dimensional case. Ω is the azimuthal angle about the vertical line through the point disturbance. The v velocity and the y co-ordinate are again stretched by the factor α^{-1} and the scale factors are $h_1 = 1-\alpha y\, d\theta/dx$, $h_2 = 1$ and $h_3 = R(x)-\alpha y \sin\theta$, where $R(x)$ is the horizontal distance from the axis to the wave path and is given by

$$R(x) = \int_0^x \cos\theta(k)\, dk.$$

The analysis now follows the two-dimensional case and it is found that the wave path, the wave profiles and the wave width are identical to the two-dimensional ones. Only the magnitudes of the dependent variables are affected and these are essentially multiplied by the factor $R^{-\frac{1}{2}}$. The dependent variables are given by

$$p_1 = \mathscr{R}\{l(r_1 \cot\theta/R)^{\frac{1}{2}} f e^{-it}\},$$

$$u_1 = \mathscr{R}\left(-\frac{il}{b}(Rr_1\cot\theta)^{-\frac{1}{2}}\frac{df}{d\eta}e^{-it}\right),$$

$$v_1 = \mathscr{R}\left\{\frac{i}{R}\left[\frac{l}{b}\left(\frac{R\tan\theta}{r_1}\right)^{\frac{1}{2}}\frac{db}{dx}\eta\frac{df}{d\eta} - \frac{d}{dx}\left(l\left(\frac{R\tan\theta}{r_1}\right)^{\frac{1}{2}}\right)f\right]e^{-it}\right\},$$

$$\rho_1 = \mathscr{R}\left\{\frac{l}{b\sin\theta}\left(\frac{r_1\tan\theta}{R}\right)^{\frac{1}{2}}\frac{df}{d\eta}e^{-it}\right\},$$

where l, b and f take their two-dimensional forms.

REFERENCES

GORDON, D. & STEVENSON, T. N. 1972 *J. Fluid Mech.* **56**, 629.

GÖRTLER, H. 1943 *Z. angew. Math. Mech.* **23**, 65.

THOMAS, N. H. & STEVENSON, T. N. 1972 *J. Fluid Mech.* **54**, 495.